Mechanical Properties of Poly(ε-caprolactone) and Poly(lactic acid) Blends

C. L. Simões,[1,2] J. C. Viana,[1,2] A. M. Cunha[1,2]

[1]*Institute for Polymers and Composites (IPC), Department of Polymer Engineering, University of Minho, Campus de Azurém, 4800-058 Guimarães, Portugal*
[2]*Innovation in Polymer Engineering (PIEP), Campus de Azurém, 4800-058 Guimarães, Portugal*

Received 26 April 2008; accepted 4 August 2008
DOI 10.1002/app.29425
Published online 29 December 2008 in Wiley InterScience (www.interscience.wiley.com).

ABSTRACT: The aim of this work was to better understand the performance of binary blends of biodegradable aliphatic polyesters to overcome some limitations of the pure polymers (e.g., brittleness, low stiffness, and low toughness). Binary blends of poly(ε-caprolactone) (PCL) and poly(lactic acid) (PLA) were prepared by melt blending (in a twin-screw extruder) followed by injection molding. The compositions ranged from pure biodegradable polymers to 25 wt % increments. Morphological characterization was performed with scanning electron microscopy and differential scanning calorimetry. The initial modulus, stress and strain at yield, strain at break, and impact toughness of the biodegradable polymer blends were investigated. The properties were described by models assuming different interfacial behaviors (e.g., good adhesion and no adhesion between the dissimilar materials). The results indicated that PCL behaved as a polymeric plasticizer to PLA and improved the flexibility and ductility of the blends, giving the blends higher impact toughness. The strain at break was effectively improved by the addition of PCL to PLA, and this was followed by a decrease in the stress at break. The two biodegradable polymers were proved to be immiscible but nevertheless showed some degree of adhesion between the two phases. This was also quantified by the mechanical property prediction models, which, in conjunction with material property characterization, allowed unambiguous detection of the interfacial behavior of the polymer blends. © 2008 Wiley Periodicals, Inc. J Appl Polym Sci 112: 345–352, 2009

Key words: biopolymers; blends; mechanical properties; modeling

INTRODUCTION

Each year, tons of petroleum-based synthetic plastics are disposed worldwide, causing environmental problems. This number has the tendency to increase each year with the increasing production and utilization of plastic-based products. Recycling and recovery activities are still very limited in the plastic sector, and this makes a landfill site the final destination for most of the used items, such as packaging, bottles, and molded products. Landfill space is becoming extremely limited and represents considerable environmental pollution issues, such as soil and water contamination. Therefore, waste management has become a major concern throughout the world, triggering general environmental awareness. With this not so positive picture, biodegradable polymers are gaining more and more attention because they can be degraded in the environment by the action of naturally occurring microorganisms. Another important factor is that most biodegradable polymers are based on renewable resources (e.g., corn, soy beans, and other crops). Aliphatic polyesters are the most known and studied biodegradable polymers, including poly(lactic acid) (PLA),[1–3] poly(ε-caprolactone) (PCL),[1,4] poly(hydroxybutyrate),[1,4–6] and poly(butylene succinate).[7,8] These materials have a large field of application,[4,9,10] with medical care,[11–15] agriculture,[16–18] and packaging[19,20] being the most widely researched areas.

Biodegradable polymers can be processed by traditional thermoplastic processing methods, and composting is a sustainable option for their disposal. These materials are not yet broadly used in industry because of their high cost and limited performance for many applications. The influence of biodegradation on the reduction of the mechanical properties of biodegradable polymers, as well as their blends and composites, has been investigated.[7,8,21] Nowadays, biodegradable polyesters are extensively studied as matrix materials in biocomposites reinforced with various natural fibers,[22–25] such as flax, sisal, hemp, jute, ramie, abaca, and chitin,[26] for improving their performance. The achievement of a completely

Correspondence to: C. L. Simões (carla.simoes@piep.pt).
Contract grant sponsor: European Commission (through the 6th Framework Program within the Custom, Environment, and Comfort Made Shoe project); contract grant number: ISTNMP 2004.

biodegradable, natural resource based material is expected. Blending biodegradable polymers can also be an approach to overcoming some limitations of single applications of these materials, such as brittleness, low stiffness, and low toughness. Some studies have evaluated the mechanical properties of biodegradable polymer blends.[27–32] Chen et al.[29] showed that the elongation of PLA increased with the addition of PCL, but the stress decreased at the same time. Broz et al.[30] suggested that PLA and PCL are not miscible and that some adhesion may occur at the PLA/PCL interface when the majority phase is PCL but not when it is PLA. Interfacial tension is an important factor affecting the compatibility of blends of biodegradable polyesters with other materials.[33]

Various methods are used for interfacial characterization between different materials (e.g., perfect adhesion and no adhesion), the technique most often used being scanning electron microscopy (SEM).[25,28,31] Other approaches have been also published, including dynamic viscoelasticity[25] and measurements of blend mechanical properties.[29] Interfacial behavior depends on a number of factors, including the interfacial tension and processing conditions, with the detection of interfacial behavior between dissimilar materials being complex. Predictive models developed by several authors[30,34] offer an expedient approach for recognizing and quantifying to some extent the interfacial behavior of polymer blends.

In this study, a series of blends of biodegradable polymers using PCL and PLA were prepared by the variation of the mass fraction across the composition range. Morphological characterization was performed with SEM and differential scanning calorimetry (DSC). The initial modulus, stress and strain at yield, strain at break, and impact toughness of the biodegradable polymer blends were investigated. The properties were described by models assuming different interfacial behaviors (e.g., good adhesion and no adhesion between the dissimilar materials), which, in conjunction with material property characterization, allowed unambiguous detection of the interfacial behavior of the polymer blends.

EXPERIMENTAL

Materials

PCL [Tone P-767; melt flow index (190°C, 0.30 MPa) = 30 g/10 min, density at 23°C = 1.145 g/cm^3] was supplied by Dow Chemical Co. (Midland, MI). PLA [Hycail HM 1010; melt flow index (190°C, 2.16 kg) = 3–8 g/10 min, density at 23°C = 1.24 g/cm^3] was purchased from Hycail B.V. (Noordhorn, The Netherlands). The specific optical rotation of PLA, $[\alpha]_D^{25}$, was −150 in chloroform at a concentration of 1 g/dL and 25°C (AA-1000 polarimeter, Cambridgeshire, England). PLA was estimated to have an L-lactide content of 96.3% under the assumption that $[\alpha]_D^{25}$ of poly(L-lactic acid) and poly(D-lactic acid) was −156 and +156, respectively.[35]

TABLE I
Injection-Molding Processing Conditions for ASTM Tensile Specimens (ASTM Charpy Impact Specimens) for the Different Blends

	PCL/PLA	
Weight ratio (wt %)	Cylinder temperature (°C)	Injection speed (mm/s)
100/0	80–95 (80–90)	50 (5)
75/25	100–120 (100–120)	50 (10)
50/50	135–180 (135–180)	10 (20)
25/75	165–180 (165–180)	15 (10)
0/100	170–200 (170–200)	30 (30)

Sample preparation

PLA was dried in an oven at 80°C for at least 4 h before processing because it is a highly hygroscopic thermoplastic and absorbs moisture from the atmosphere. Blends of different weight ratios, ranging from pure biodegradable polymers to 25 wt % increments, were prepared by extrusion in a Carvex (Lisbon, Portugal) counter-rotating twin screw machine with a screw diameter of 52 mm, a length/diameter ratio of 18, and a 15-mm double circular die. The cylinder temperatures rose from 160 to 170°C, and the screw speed was around 20 rpm. The blend threads were cut into small pieces and cooled in water until solidification. After cooling and drying at the ambient temperature, the material was granulated in a Colortronic (Derbyshire, UK) M102L cutting mill. The obtained pellets of the biodegradable polymer blends were processed by injection molding into ASTM D 638-99 tensile specimens and ASTM D 256-87 Charpy impact specimens in an Engel (Schwertberg, Austria) ES45 HL-V machine (45 kN clamping force). The processing conditions were adjusted for each blend and specimen geometry (Table I).

Characterization

DSC

Morphology analysis was carried out by DSC on a TA Instruments (New Castle, DE) Q20 differential scanning calorimeter. DSC scans were performed with samples obtained from injected specimens that were heated from 20 to 180°C at a rate of 20°C/min. The crystallinity degree of PCL ($X_{c,\ PCL}$) in the blends was calculated from eq. (1) with consideration of the amount of PCL in the blend.[36] For PCL, a

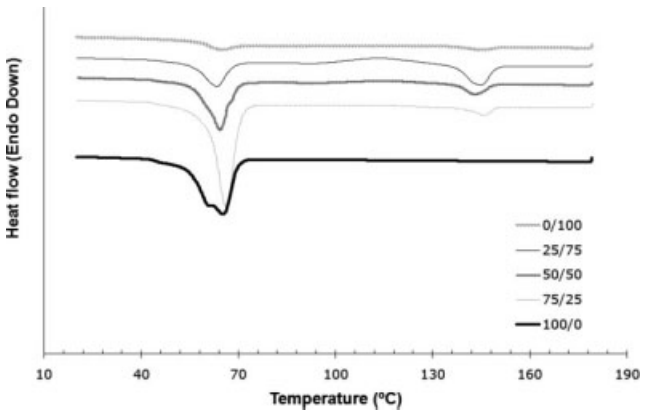

Figure 1 DSC scan thermograms of the PCL, PLA, and PCL/PLA blends.

100% crystalline melting enthalpy ($\Delta H_{0,\mathrm{PCL}}$) of 156.8 J/g[37] was assumed. For PLA, the crystallinity degree ($X_{c,\mathrm{PLA}}$) was calculated from eq. (2), and for PLA, the 100% crystalline melting enthalpy ($\Delta H_{0,\mathrm{PLA}}$) was taken to be 93 J/g:[27]

$$X_{c,\mathrm{PCL}}(\%) = \left[\frac{\Delta H_{m,\mathrm{PCL}}}{\Delta H_{0,\mathrm{PCL}} W_{\mathrm{PCL}}}\right] \times 100 \qquad (1)$$

$$X_{c,\mathrm{PLA}}(\%) = \left[\frac{\Delta H_{m,\mathrm{PLA}} - \Delta H_{cc,\mathrm{PLA}}}{\Delta H_{0,\mathrm{PLA}} W_{\mathrm{PLA}}}\right] \times 100 \qquad (2)$$

where W_{PCL} and W_{PLA} are the weight fractions of PCL and PLA in the blends, respectively; $\Delta H_{m,\ \mathrm{PCL}}$ and $\Delta H_{m,\mathrm{PLA}}$ are the melting enthalpies of PCL and PLA in the blends, respectively; and $\Delta H_{cc,\mathrm{PLA}}$ is the cold crystallization enthalpy of PLA in the blends. The presented results are averages of three samples.

Mechanical characterization

Tensile and Charpy impact tests were performed to characterize the mechanical behavior of the biodegradable polymers blends. The tensile tests were performed in accordance with ASTM D 638-99 on an Instron (Norwood, MA) 4505 universal testing machine with a 50 kN load cell. The initial modulus, stress and strain at yield, and stress at break were assessed. During the determination of the modulus, an extensometer with a 50-mm gauge length and a 2 mm/min crosshead speed was used. A crosshead speed of 50 mm/min was used for the determination of the other mechanical properties. The Charpy impact tests were performed in accordance with ASTM D 256-87 on a Ceast (Pianezza, Italy) machine with a pendulum energy of 2 J or 4 J, depending on the polymer blend, and the impact toughness was calculated. All performed tests were carried out in a standard laboratory atmosphere of 23°C and 50% relative humidity.

SEM

The fracture surfaces of the injection-molded impact bars were observed with SEM. The fractured surface was sputtered with a thin layer of gold before imaging on a Leica (Wetzlar, Germany) S360 scanning electron microscope.

RESULTS AND DISCUSSION

DSC

The crystalline structure and melting of the samples were characterized with DSC because crystallinity plays an important role in the mechanical properties of the systems. Selected heating thermograms of PCL, PLA, and PCL/PLA blends are shown in Figure 1. Pure PCL has a crystallinity of approximately 43% and a melting temperature of approximately 74°C. The glass transition is around −60°C; therefore, it was not detected in the scans. Pure PLA has a crystallinity of less than 2%, and it can be assumed to be amorphous and have a glass-transition temperature of 59°C and a melting temperature of approximately 145°C. The immiscibility of the two materials is confirmed by the DSC scans of the blends, which show two independent melting peaks corresponding to PCL (at ca. 65°C) and PLA (at ca. 145°C).

The melting enthalpies of the pure biodegradable polymers and their blends were calculated, as well as the cold crystallization enthalpy of PLA. The peak melting temperature across the composition range for PCL/PLA blends is shown in Figure 2. The addition of PLA reduces the melting temperature of the PCL phase, and this indicates the development of thinner lamellae of PCL. The addition of up to 50% PCL decreases the melting temperature of the PLA phase. Thereafter, the melting temperature of PLA increases as PLA lamellae become thicker, possibly because of a nucleation effect of PCL.

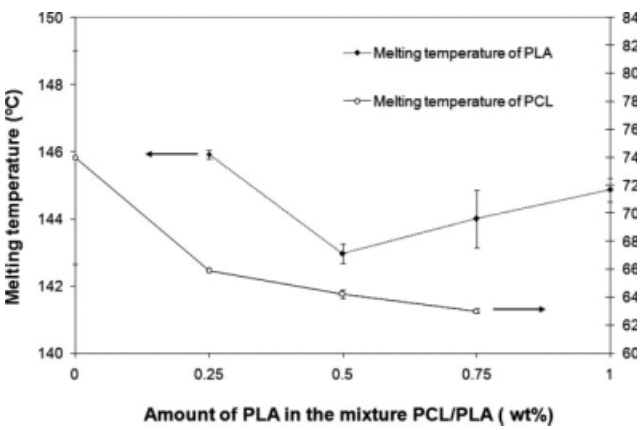

Figure 2 Variation of the melting temperature for PCL, PLA, and their blends.

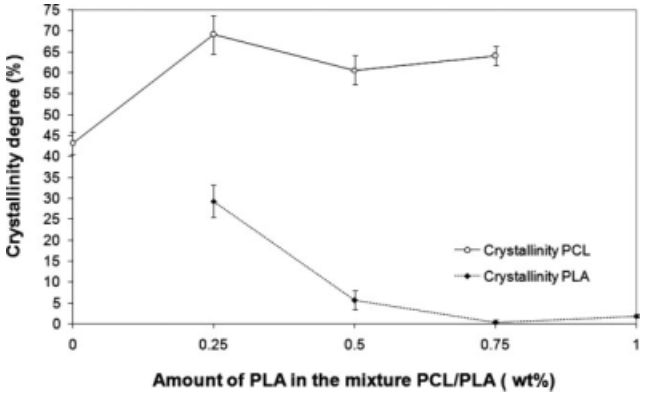

Figure 3 Variation of the degree of crystallinity of the PCL and PLA phases in PCL/PLA blends.

The crystallinity of PCL and PLA in the blends is shown in Figure 3. The relative degree of crystallinity of the PLA phase increases with the addition of PCL, and this suggests that PCL promotes the crystallization of the PLA phase. Adding PCL to PLA increases the crystallinity of PLA (nucleation effect), reducing the thickness of the PLA lamellae. The relative degree of crystallinity of the PCL phase increases with the addition of up to 25 wt % PLA. Further addition of PLA does not significantly change the crystallinity of PCL. The addition of PLA to PCL increases the crystallinity of PCL, increasing the thickness of PCL lamellae (thicker lamellae).

Mechanical characterization

Typical stress–strain curves of PCL, PLA, and PCL/PLA blends are shown in Figure 4. During the tensile tests, it was verified that none of the specimens of PCL or the 75/25 PCL/PLA blend had failed. The tests were stopped at the maximum displacement of the tensile machine, which corresponded to a strain of 375%. Therefore, these materials exhibit a strain at break higher than 375%. PLA shows a higher initial modulus and strain at break than PCL but a lower

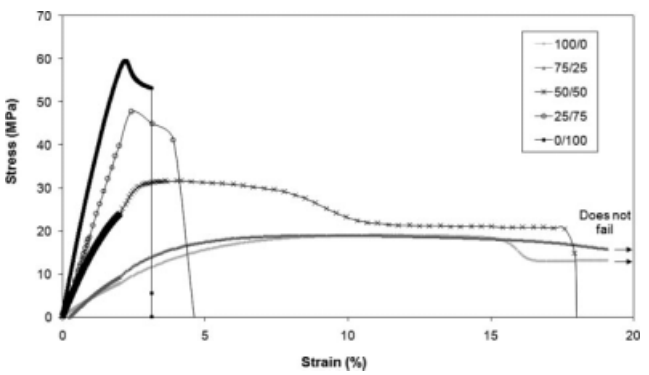

Figure 4 Typical stress–strain curves of PCL/PLA blends.

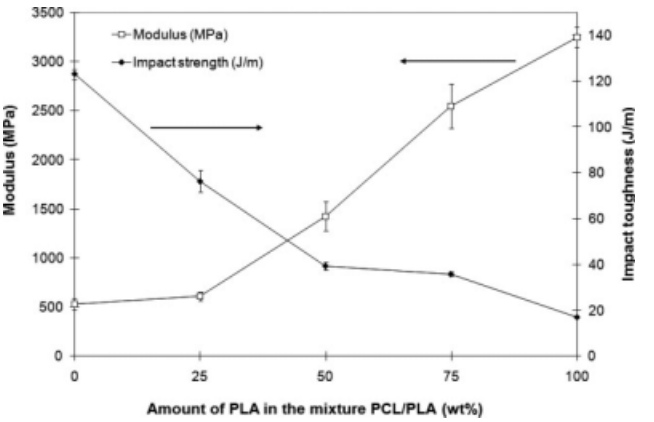

Figure 5 Tensile properties and impact toughness of PCL, PLA, and PCL/PLA blends: initial modulus (MPa) and impact toughness (J/m).

deformation capability, as expected. The addition of PCL to PLA reduces the initial modulus and the maximum stress level but increases considerably the strain at break.

In general, PCL acts as a polymeric plasticizer, lowering the initial modulus and yield stress, increasing the strain at yield and at break, and enhancing the flexibility and ductility of a blend. The addition of PCL gives blends higher impact toughness, decreasing the brittleness of the materials. Figure 5 shows the initial modulus and impact toughness for PCL, PLA, and their blends as functions of the mass fraction of PLA (wt %), presenting average experimental data scattering of 8 and 3%, respectively.

The increase in the initial modulus of the PCL/PLA blends with the addition of PLA is lower for the lower increments of PLA. Until 25% PLA, the initial modulus remains almost constant, close to the initial modulus of PCL. The impact toughness of PLA decreases almost linearly with the addition of PCL.

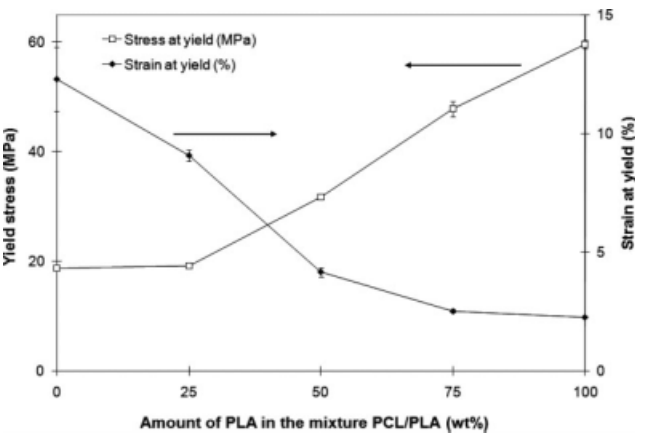

Figure 6 Tensile properties of PCL, PLA, and PCL/PLA blends: yield stress (MPa) and strain at yield (%).

Figure 6 shows the stress and strain at yield across the composition range for PCL/PLA blends as functions of the mass fraction of PLA (wt %), presenting average experimental data scattering of approximately 1 and 4%, respectively. The strain at yield decreases with the addition of PLA; after 75% PLA, it remains almost constant, close to the strain at yield of PLA. The yield stress increases with the addition of PLA; until 25% PLA, it remains almost constant, close to the yield stress of PCL.

Prediction models

The mechanical properties of the blends (indicated by subscript b) were described by models assuming different interfacial behaviors between dissimilar materials (e.g., models for perfect adhesion and no adhesion).

Initial modulus

The variations of the initial modulus were compared with theoretical predictions using different models. The rule of mixture [eq. (3)] considers perfect adhesion between the matrix and the dispersed phase (indicated by subscript d) and perfect dispersion of the spherical inclusions in the matrix:

$$E_b = \left(\left[\frac{E_d}{E_m} - 1\right] \times \phi_d + 1\right) \times E_m \tag{3}$$

where E_b is the initial modulus of the bend, E_d is the initial modulus of the disperse phase, E_m is the initial modulus of the matrix, and ϕ_d is the volume fraction of the disperse phase.

In the foam model proposed by Cohen and Ishai [eq. (4)], the disperse phase is considered a noninteracting phase equivalent to a void or pore:[34]

$$E_b = \left(1 - \phi_d^{2/3}\right) \times E_m \tag{4}$$

The Kerner–Uemura–Takayanagi (KUT) model [eqs. (5) and (6)] treats the blends as spherical inclusions of one polymer having E_d in a continuous matrix of another polymer having E_m, and Poisson's ratio of the matrix (ν_m) is taken to be 0.5.[30] This model has two variations. One assumes perfect adhesion at the blend interface [eq. (5)], and the other assumes no adhesion [eq. (6)]:

$$E_b = E_m\left(\frac{(7 - 5\upsilon_m) \times E_m + (8 - 10\upsilon_m) \times E_d - (7 - 5\upsilon_m)(E_m - E_d) \times \phi_d}{(7 - 5\upsilon_m) \times E_m + (8 - 10\upsilon_m) \times E_d + (8 - 10\upsilon_m)(E_m - E_d) \times \phi_d}\right) \tag{5}$$

$$E_b = E_m\left(\frac{(7 - 5\upsilon_m) \times E_m - (7 - 5\upsilon_m) \times E_m\phi_d}{(7 - 5\upsilon_m) \times E_m + (8 - 10\upsilon_m) \times E_m\phi_d}\right) \tag{6}$$

In the calculations, it was assumed that for PCL mass fractions less than or equal to 50 wt % (volume fraction of 0.48), PLA formed the continuous matrix (indicated by subscript m), and above 50 wt %, PCL was the matrix.

Figure 7 presents the variation of the initial modulus of PCL, PLA, and their blends and the predictive models: the rule of mixture, the foam model, and the KUT model.

The initial modulus of the blends follows the rule of mixture up to 25 wt % PCL, and this indicates some adhesion between the two phases in this composition range. In this case, it is assumed that PLA is the continuous matrix and PCL is the dispersed phase. In the composition with up to 25 wt % PCL, the initial modulus follows the KUT model more closely for perfect adhesion between the blend components. The foam model and the no-adhesion KUT model both assume no adhesion between the blend components, and they show similar trends, as expected, because both are based on the assumption that the dispersed phase is a noninteracting phase behaving as a void or pore. The deviation from the models indicates some degree of interaction between the two phases for low strains.

Yield stress

The variations of the experimental values of the yield stress were compared with theoretical

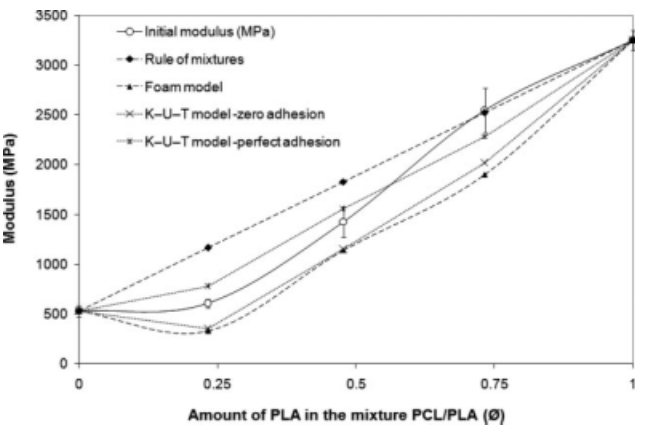

Figure 7 Variation of the initial modulus of PCL, PLA, and PCL/PLA blends and the predictive models: the rule of mixture [eq. (3)], the foam model [eq. (4)], and the KUT models [eqs. (5) and (6)].

TABLE II
Values of K and α for PCL/PLA Blends

	PCL/PLA	
PLA volume fraction	K	α
0	0	0
0.23	−0.05	−0.08
0.48	0.72	1.21
0.73	0.48	0.82
1	0	0
Average	0.6	1

predictions using different models. In the rule of mixture [eq. (7)]

$$\sigma_b = \left(\left[\frac{\sigma_d}{\sigma_m} - 1\right] \times \phi_d + 1\right) \times \sigma_m \quad (7)$$

where σ_b is the yield stress of the bend, σ_d is the yield stress of the disperse phase, and σ_m is the yield stress of the matrix.

In the Nicolais–Narkis (NN) model [eq. (8)], the interphase interaction constant (K) is a function of the blend structure. For spherical inclusions, $K = 1.21$ stands for the extreme case of poor adhesion; interphase adhesion takes place for values of $K < 1.21$: the lower the value, the better the adhesion. $K = 0$ is considered for sufficient adhesion so that the polymer matrix strength does not decrease:[34]

$$\sigma_b = \left(1 - K\phi_d^{2/3}\right) \times \sigma_m \quad (8)$$

In the porosity model [eq. (9)], the weakness in the structure or stress concentration is described by the stress concentration parameter α. The higher the α value is, the higher the extent is of stress concentration and thus the higher the decrease is in the yield stress.[34] This model assumes that the disperse phase is equal to pores/voids in the matrix. The pores or voids do not influence the mechanical properties of the two-phase systems because of no adhesion at the phase boundaries but acts as a stress concentration:

$$\sigma_b = ([\exp(-\alpha\phi_d)]) \times \sigma_m \quad (9)$$

In the Béla–Pukánszky (BP) model [eq. (10)], the tensile yield stress of the blend is determined by the yield stress of the matrix, the effective load-bearing cross section, and the interaction. B is a parameter related to the load-bearing capacity of the disperse phase and depends on the size of the contact surface between the polymer and the disperse phase and on the properties of the interphase that is formed. Aggregation decreases the surface available for the polymer, and consequently, the value of B should also decrease:[38]

$$\sigma_b = \sigma_m \left(\frac{1 - \phi_d}{1 + 2.5\phi_d}\right) \times \exp(B\phi_d) \quad (10)$$

The NN model and the porosity model assume that both phases are of a no-adherent type and the yield stress is a function of either the area fraction or the volume fraction of the dispersed phase.[34] Table II presents the values of K and α for each ϕ_d value; they were determined by a comparison of the experimental yield stress data with the models. Because of data scatter, the average value was estimated, excluding K and α at $\phi_d = 0.23$.

According to the NN model, the values of K are less than unity, with an average value of 0.6, indicating some degree of adhesion and a smaller amount of weakness of the blend structure. The porosity model presents an average α value of 1, revealing some amount of stress concentration. Figure 8 presents the variation of the yield stress of PCL, PLA, and their blends and the predictive models: the rule of mixture and NN model for K values of 0.6 and 1.21.

Figure 9 presents the variation of the yield stress of PCL, PLA, and their blends and the predictive models: the rule of mixture and the porosity model for $\alpha = 1$.

The yield stress follows the rule of mixture up to 25 wt % PCL, indicating some adhesion between the two phases in this composition range. The overall yield stress data show a good fit to both the NN model and the porosity model, with an average K value of 0.6 (Fig. 8) and an average α value of 1 (Fig. 9); this indicates a degree of adhesion between the phases.

According to the BP model, when the disperse phase is PLA, B is approximately 3.2, and when the disperse phase is PCL, it is 1.9; this indicates that interphase adhesion is promoted when PCL is the matrix.

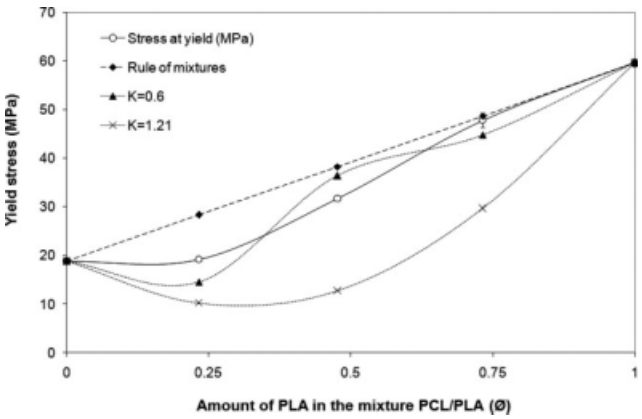

Figure 8 Variation of the yield stress of PCL, PLA, and PCL/PLA blends and the predictive models: the rule of mixture [eq. (7)] and the NN model [eq. (8)].

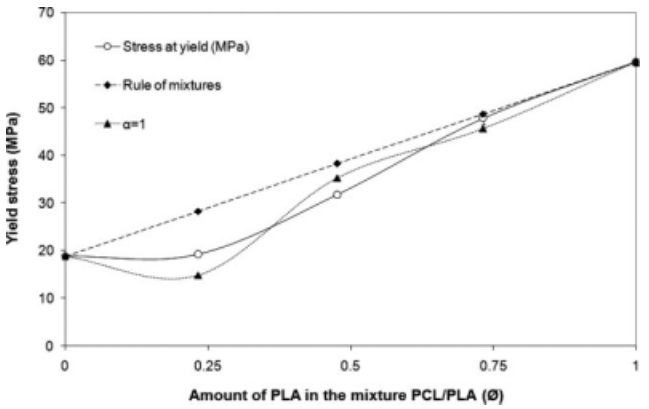

Figure 9 Variation of the yield stress of PCL, PLA, and PCL/PLA blends and the predictive models: the rule of mixture [eq. (7)] and the porosity model [eq. (9)].

SEM

The fracture surfaces of pure biodegradable polymers and PCL/PLA blends were observed with SEM. Figure 10(a–f) shows the SEM micrographs of PCL, PLA, and PCL/PLA blends. The PLA's fracture surface shows a more brittle material, as confirmed by the tensile and Charpy impact tests. Phase separation was shown by all PCL/PLA blends, confirming that the two biodegradable polymers are immiscible. The second phase has spherical geometry and is well dispersed in the matrix. Phase inversion takes place when the PCL content is at least less than 50 wt %. The dispersed PLA spheres of the 75/25 blend present a smaller diameter than the PCL spheres of the 25/75 blend because of the different viscosities of the two materials. The PLA

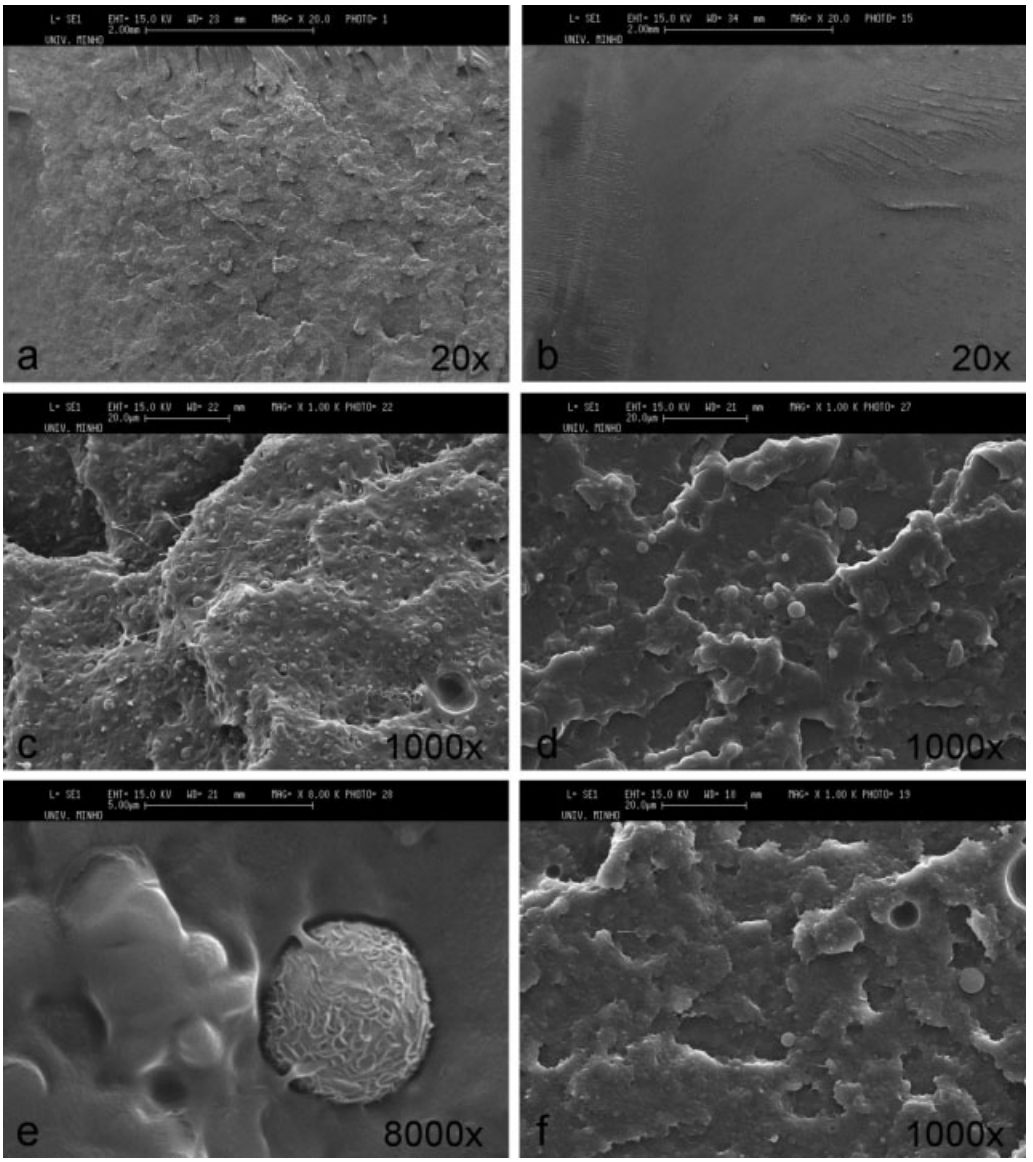

Figure 10 SEM micrographs of the fracture surfaces of injected molded specimens: (a) PCL, (b) PLA, (c) 75/25 PCL/PLA blend, (d,e) 50/50 PCL/PLA blend, and (f) 25/75 PCL/PLA blend.

inclusions show some degree of deformation, indicating some adhesion between the two polymers.

CONCLUSIONS

The properties of biodegradable polymers such as PCL and PLA can be tailored to achieve a given performance. The addition of PCL lowers the initial modulus and yield stress; it behaves as a polymeric plasticizer and enhances the flexibility and ductility of the blend. PCL gives the blends higher impact toughness, decreasing the brittleness of the materials. The strain at break is effectively improved by the addition of PCL to PLA, and this is followed by a decrease in the stress at break. Phase separation was revealed by all PCL/PLA blends in the SEM studies, and DSC results have confirmed that the two biodegradable polymers are immiscible. A second phase with a spherical geometry was seen to be dispersed in the matrix but nevertheless showed some degree of adhesion between the two phases. This was also indicated by the mechanical property prediction model analyses, which also showed that this phenomenon is promoted when PCL is the matrix. Prediction models and material property characterization allowed unambiguous detection of the interfacial behavior of the polymer blends.

References

1. Van de Velde, K.; Kiekens, P. Polym Test 2002, 21, 433.
2. Lunt, J. Polym Degrad Stab 1998, 59, 145.
3. Kunioka, M.; Ninomiya, F.; Funabashi, M. Polym Degrad Stab 2006, 91, 1919.
4. Chandra, R.; Rustgi, R. Prog Polym Sci 1998, 23, 1273.
5. Reddy, C. S. K.; Ghai, R.; Rashmi, K. V. C. Bioresour Technol 2003, 87, 137.
6. Khanna, S.; Srivastava, A. K. Process Biochem 2005, 40, 607.
7. Kim, H. S.; Yang, H. S.; Kim, H. J. J Appl Polym Sci 2005, 97, 1513.
8. Kim, H. S.; Kim, H. J.; Lee, J. W.; Choi, I. G. Polym Degrad Stab 2006, 91, 1117.
9. Amass, W.; Amass, A.; Tighe, B. Polym Int 1998, 47, 89.
10. Ikada, Y.; Tsuji, H. Macromol Rapid Commun 2000, 21, 117.
11. Reis, R. L.; Cunha, A. M. J Mater Sci: Mater Med 1995, 6, 786.
12. Sousa, R. A.; Kalay, G.; Reis, R. L.; Cunha, A. M.; Bevis, M. J. J Appl Polym Sci 2000, 77, 1303.
13. Vaz, C. M.; Van Doeveren, P. F. N. M.; Reis, R. L.; Cunha, A. M. Polymer 2003, 44, 5983.
14. Winzenburg, G.; Schmidt, C.; Fuchs, S.; Kissel, T. Adv Drug Delivery Rev 2004, 56, 1453.
15. Kim, H. W.; Knowles, J. C.; Kim, H. E. Biomaterials 2004, 25, 1279.
16. Biodegradable Polymers for Industrial Applications; Smith, R., Ed.; Woodhead: Cambridge, England, 2005.
17. Prisco, N. D.; Immirzi, B.; Malinconico, M.; Mormile, P.; Petti, L.; Gatta, G. J Appl Polym Sci 2002, 86, 622.
18. Briassoulis, D. Polym Degrad Stab 2006, 91, 1256.
19. Plackett, D. V.; Holm, V. K.; Johansen, P.; Ndoni, S.; Nielsen, P. V.; Sipilainen-Malm, T.; Södergård, A.; Verstichel, S. Packag Technol Sci 2006, 19, 1.
20. Davis, G.; Song, J. H. Ind Crops Prod 2006, 23, 147.
21. Reis, R. L.; Mendes, S. C.; Cunha, A. M.; Bevis, M. J. Polym Int 1997, 43, 347.
22. Wollerdorfer, M.; Bader, H. Ind Crops Prod 1998, 8, 105.
23. Mohanty, A. K.; Misra, M.; Drzal, L. T. J Polym Environ 2002, 10, 19.
24. Zini, E.; Baiardo, M.; Armelao, L.; Scandola, M. Macromol Biosci 2004, 4, 286.
25. Shibata, M.; Ozawa, K.; Teramoto, N.; Yosomiya, R.; Takeishi, H. Macromol Mater Eng 2003, 288, 35.
26. Chen, B.; Sun, K.; Ren, T. Eur Polym J 2005, 41, 453.
27. Shibata, M.; Inoue, Y.; Miyoshi, M. Polymer 2006, 47, 3557.
28. Duarte, M. A. T.; Hugen, R. G.; Martins, E. S. A. Mater Res 2006, 9, 25.
29. Chen, C. C.; Chueh, J. Y.; Tseng, H.; Huang, H. M.; Lee, S. Y. Biomaterials 2003, 24, 1167.
30. Broz, M.; VanderHart, D.; Washburn, N. Biomaterials 2003, 24, 4181.
31. Correlo, V. M.; Boesel, L. F.; Bhattacharya, M.; Mano, J. F.; Neves, N. M.; Reis, R. L. Mater Sci Eng A 2005, 403, 57.
32. Lee, S.; Lee, J. W. Korea-Aust Rheol J 2005, 17, 71.
33. Biresaw, G.; Carriere, C. J. Compos A 2004, 35, 313.
34. Tomar, N.; Maiti, S. N. J Appl Polym Sci 2007, 104, 1807.
35. Hu, Y.; Hu, Y. S.; Topolkaraev, V.; Hiltner, A.; Baer, E. Polymer 2003, 44, 5711.
36. Ghaffar, A. M. E. H. A. Ph.D. Thesis, University of Halle, 2002.
37. Schick, C.; Merzlyakov, M.; Minakov, A.; Wurm, A. J Therm Anal Calorim 2000, 59, 279.
38. Kiss, A.; Fekete, E.; Pukánszky, B. Compos Sci Technol 2007, 67, 1574.